JOURNAL OF CATALYSIS 98, 51–63 (1986)

Co/Mo/Alumina Catalyst Structure Determination by EXAFS

III. The Catalysts: Their Preparation, Characterization, and HDS Activities

MARVIN F. L. JOHNSON,*,[1] ANDREW P. VOSS,* S. H. BAUER,† AND N-S. CHIU†

*ARCO Petroleum Products Company, Harvey Technical Center, Harvey, Illinois 60426; and †Department of Chemistry, Cornell University, Ithaca, New York 14853

Received April 2, 1985; revised September 17, 1985

A series of Co/Mo/alumina hydrodesulfurization catalysts was prepared following standard procedures, to generate an internally consistent set, wherein the content of the metal atoms was varied in a regular manner. The range in Mo compositions was 2 → 30%; the range in Co content was 0 → 12%. These preparations were fully characterized in the oxide state by measurements of the surface areas, pore-size distributions, diffuse reflectance spectra, and an occasional Raman spectrum. Standard activity tests were then run with light cycle oil. These values are empirically correlated with other physical characterizations which primarily involve the compositions and surface areas. Activity tests were also run for several commercial catalysts, following a variety of regeneration and sulfurization protocols. The objective was to develop a rational model for relating activity to molecular structure, as determined from EXAFS spectra in the oxide and sulfide states.

INTRODUCTION

In the first paper (*1*) of this series we presented results derived from EXAFS spectra at the Mo K-edge, of a number of Co/Mo/alumina catalysts in the oxidized state, having MoO_3 levels up to 30%, and CoO as high as 12%. The EXAFS spectra were reduced to radial distribution curves by means of an improved procedure (*2*). These data and other information in the literature led to a model for the surface structure which consists of distorted MoO_6 octahedra.

In this paper we describe the preparations of the above catalysts, their characterizations by conventional techniques of pore distribution (PD), X-ray diffraction (XRD), and UV diffuse reflectance, and the results of hydrodesulfurization (HDS) activity measurements. For the HDS work, a petroleum fraction was used under conditions which realistically simulate operations in a commercial HDS unit. The structures of these sulfided catalysts derived from EXAFS spectra at the Mo K-edge are presented in an accompanying paper (*3*). From these analyses a relationship between HDS activity and the state of MoS_2 was developed.

EXPERIMENTAL

A. Catalyst Preparations

The base for most of these preparations was a powdered alumina from Conoco, designated Catapal. This alumina as received was found by XRD to be essentially pure boehmite alumina monohydrate, which converted to essentially pure γ-alumina by calcination. It was extruded, dried, and calcined in flowing air at 550°C. The product had a surface area of 289 m^2/g, and a total pore volume of 0.552 cm^3/g. Portions of this alumina were impregnated with ammonium molybdate solutions by the incipient wetness technique, and again calcined

[1] Present address: 1124 Elder Rd., Homewood, Ill., 60430.

0021-9517/86 $3.00

in flowing air at 550°C to give preparations having up to 30% MoO_3, in 6% increments. Two similar preparations with 2 and 4% MoO_3 were used only for EXAFS studies. Portions of each of the Mo/aluminas were impregnated with cobalt nitrate solutions, dried and calcined at 550°C, to yield catalysts with 1.5, 3.0, 6.0, and 12.0% CoO.

A few preparations were made in the same manner from another alumina which consisted of about 50% boehmite in the uncalcined state, and 50% alumina after calcination, the remainder being amorphous alumina. Consequently, this was a low-area base, with 194 m^2/g. All catalyst weights used in measurements of catalytic activity or of pore distributions were corrected for ignition losses at 650°C.

In order to maintain surface area during the calcination steps, particularly when changes in area were under study, it was essential to avoid self-steaming. This can occur if the moisture driven off by rising temperatures attains too high a partial pressure. Self-steaming was minimized in this work by raising the temperature at a rate of 5°C/min, and by flowing air through the 2-in. calcination vessel at the rate of 110 liters/h, for 100 g of catalyst.

B. Pore Distribution Measurements

The pore distributions were calculated from nitrogen desorption data for pores below about 500 Å radius, and from mercury porosimetry for the macropores, with melding at about 500 Å, where the distributions are flat. When the cumulative distributions by nitrogen were calculated upward from zero, and the mercury data downward from the separately measured total pore volume, the two agreed within about 0.01 cm^3/g. The mercury data were then adjusted, usually by substraction, to give coincidence near 500 Å radius; the nitrogen data above that point and the mercury data below were discarded. The initial values of total pore volumes were measured by a He–Hg displacement technique, with a correction of 0.01 cm^3 for every 100 m^2 of surface area, to allow for the fact that the radius of the He atom is 1.0 Å.

Nitrogen desorption data were obtained using a gravimetric apparatus, which is equipped with a Cahn electrobalance to measure the quantities adsorbed, and two MKS Baratron pressure gauges to measure P and P_0. Surface areas and desorption isotherm data obtained for ASTM reference materials were in excellent agreement with round-robin results of volumetric measurements described in ASTM methods D-3663 and D-4222. The pore distribution data were calculated from the desorption isotherms in a conventional manner, starting from saturation and continuing until the calculated pore volume equaled that derived from the saturation adsorption. Cumulative surface areas ranged from 0 to 8% greater than the BET areas, averaging 3%. Mercury penetrations were measured by a Micromeritics Model 900 porosimeter, operative to 50,000 psi.

C. Reflectance Spectra

Diffuse reflectance spectra in the UV/visible region of samples ground to 60–200 mesh were recorded by a Cary Model 14M spectrophotometer. $\text{Log}(R_0/R)$ values were read at 10-nm intervals, corrected for background derived from corresponding spectra of $MgCO_3$, and the wavelengths converted to wavenumbers.

D. HDS Activity Test

The oil to be desulfurized was a Light Cycle Oil (LCO) from a commercial Fluid Catalytic Cracking unit. Some of its properties are listed in Table 1.

The HDS activity tests were carried out in a steel 1-in.-i.d., tubular downflow reactor, with 25 g of catalyst diluted with inert α-alumina. The catalyst was presulfided at 1 atm by 10% H_2S/H_2 gas flowing at a rate equivalent to 0.95 g H_2S/g of catalyst per hour for a total of 10 hours. During this period the temperature was increased from 204 to 371°C in stages. Oil flow was then started, and conditions adjusted to 400 psig

TABLE 1

Light Cycle Oil Properties

Sp. gr. at 15.6°C (g/cm³)	0.952
% S	1.20/1.23
% N	0.072
% Aromatics	74
ASTM D-86 distillation	
IBP	234°C
50%	277°C
BP	340°C

pressure, with a hydrogen rate of 2000 SCF/barrel of feed. Tests were made at two temperatures—316 and 343°C. At each of these temperatures duplicate runs were made at 2 and 6 weight hourly space velocity (WHSV). In some cases tests were also made at 3 WHSV. A total of 8–10 tests were obtained for most catalysts, allowing time for lineout when conditions were changed. Each activity run lasted 2–3 weeks. During these periods there was no decline in catalyst activity.

Hydrogen sulfide was removed from the liquid product by an on-line stripper (which separates by distillation gaseous from liquid products) located in the liquid product effluent after a gas–liquid separator. The sulfur content of feed and liquid products were determined by X-ray fluorescence. Before calculating relative activities, small adjustments were made to correct for slight deviations of the average reactor temperatures from the target temperatures. The corrections were made using previously established correlations.

Rate constants were calculated for each catalyst at each temperature, using an integrated form of the generalized rate equation governing irreversible reactions. This equation relates conversion to space-time values at a given temperature.

$$[S_p^{(1-n)} - S_f^{(1-n)}]/(n-1) = kt = k/\text{WHSV}, \quad (1)$$

where S_f = wt% sulfur in feed; S_p = wt% sulfur in product; n = reaction order; k = nth order rate constant in h^{-1}; WHSV = grams of feed per hour, per gram of catalyst.

We recognize that this is a simplified approach because a light cycle oil contains many sulfur compounds, not all of which follow the same kinetics. While it is true that thiophene and other single-component sulfur hydrocompounds can be described by a first-order equation, a complex mixture follows higher order kinetics depending on relative amounts of lumped types, and on conversion levels. For the present purposes, it was found that reasonably good fits could be obtained by using a reaction order of 2.0 for data gathered at 343°C, and a reaction order of 2.75 for those obtained at 316°C. Sulfur conversions, expressed as S_f/S_p, ranged between 1.1 and 8.3 at 316°C and between 1.4 and 25 at 343°C. Rate constants per unit of catalyst surface area (κ) are summarized in Table 2. Since the apparent reaction order at 343°C is 2, Eq. (1) reduces to

$$[S_p^{-1} - S_f^{-1}] = k/\text{WHSV}. \quad (2)$$

RESULTS

A. *Catalyst Characterizations*

All the X-ray diffraction patterns for the Catapal-based catalysts were identical to that of the base alumina, with no detectable Debye–Scherrer peaks which could be assigned to free MoO_3. This applied even at the high loading of 30% MoO_3 because of the relatively high surface area of the alumina (in comparison with most of those reported in the literature), and because of the pains taken to maintain high area in the catalysts. The sulfided samples were also amorphous, except for one weak XRD line, not identified. Clearly, bulk MoS_2 was not present in the sulfided samples.

Typical pore distribution plots are shown in Fig. 1 for molybdena on the high-area (Catapal) alumina. The total pore volume was reduced when MoO_3 was added to the extrudates, with little apparent change in pore radius. The mesopore radii of the cata-

TABLE 2

HDS Activities of Co/Mo/Catapal Alumina

%CoO	%MoO_3	Surface area (m^2/g)	HDS activity		% Sulfur[a]		
			k	κ/Area	Observed[b]	Predicted[c]	Ratio
1.5	5.7	262	13.5	0.051	2.2	3.2	0.68
3	5.8	263	13.6	0.052	3.3	3.7	0.88
6	5.6	259	12.5	0.048	4.1	4.7	0.86
1.5	11.8	265	12.8	0.048	5.1	5.7	0.89
3	11.6	267	21.9	0.082	6.0	6.2	0.97
6	11.3	263	23.8	0.091	7.3	7.5	0.98
12	10.6	228	15.6	0.068	8.7	9.0	0.96
0	18.0	256	1.3	0.0050	8.0	7.9	1.02
1.5	17.7	260	17.4	0.067	10.7	8.3	1.29
3	17.5	251	23.5	0.094	8.7	8.7	1.00
6	16.9	235	37.9	0.161	N.A.	9.5	N.A.
12	15.8	231	19.0	0.082	10.3	11.2	0.92
1.5	29.6	210	20.6	0.098	11.5	13.3	0.87
6	28.2	298	31.5	0.159	11.2	14.3	0.79

[a] Analyses of catalysts after HDS testing; expressed on ignited weight basis.
[b] By LECO method.
[c] Assuming conversion to Co_9S_8 + MoS_2.

lysts are 2–4 Å lower than that of the alumina, for which the peak in the distribution plot occurs at 33 Å, but there was no regular change in size as percentage of MoO_3 was increased. The observed change might be due to the wetting, drying, and calcination steps involved in catalyst preparations. The effects of MoO_3 content on the total pore volume and surface area of the catalysts are shown in Figs. 2 and 3, respec-

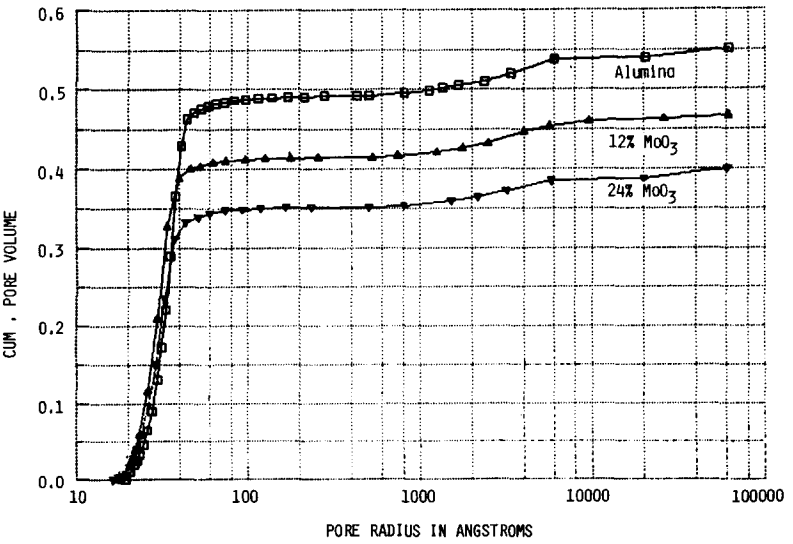

FIG. 1. Pore volume distributions, MoO_3/Catapal alumina.

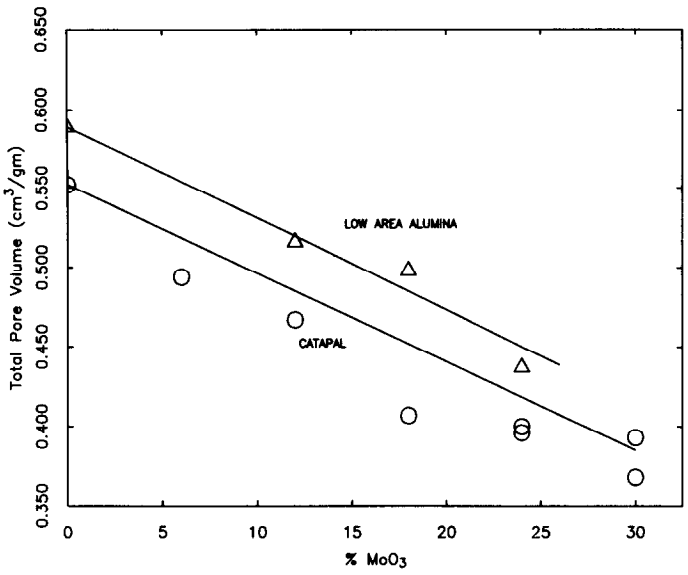

FIG. 2. Total pore volume vs molybdenum loading. The lines were calculated from values for the aluminas assuming simple dilution.

tively. The symbols are experimental values which include duplicate preparations for the higher MoO_3 levels. The lines were calculated from values for the aluminas assuming simple dilution. To a first approximation, the areas and pore volumes observed are as expected from mechanical mixtures of MoO_3 with alumina.

On a 289 m^2/g alumina support, a catalyst which incorporates 30% MoO_3 has an available area 202 m^2/g, or $\approx$16 $Å^2$ per Mo unit. In crystalline MoO_3 (d = 4.69 g/cm^3), 51 $Å^3$ is occupied by each Mo (with associated oxygen atoms), equivalent to an effective area of 13.7 $Å^2$. Hence a value of 16 $Å^2$ for the monolayer cross section of an MoO_x is

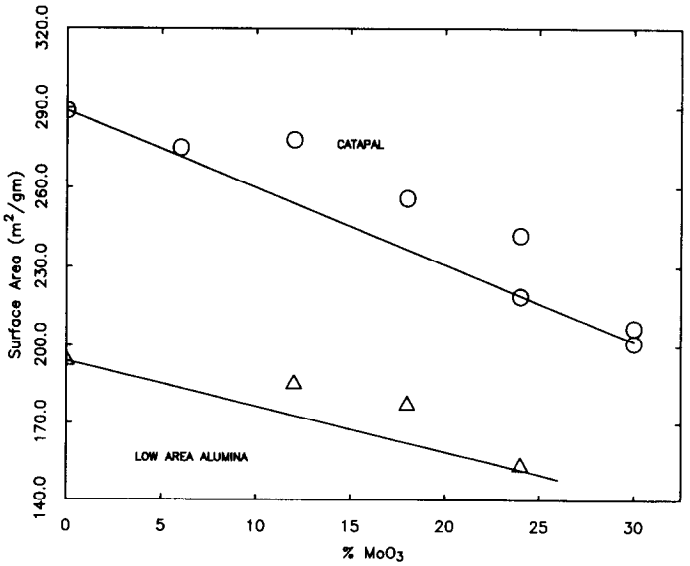

FIG. 3. Surface area vs molybdenum loading. The lines were calculated from values for the aluminas assuming simple dilution.

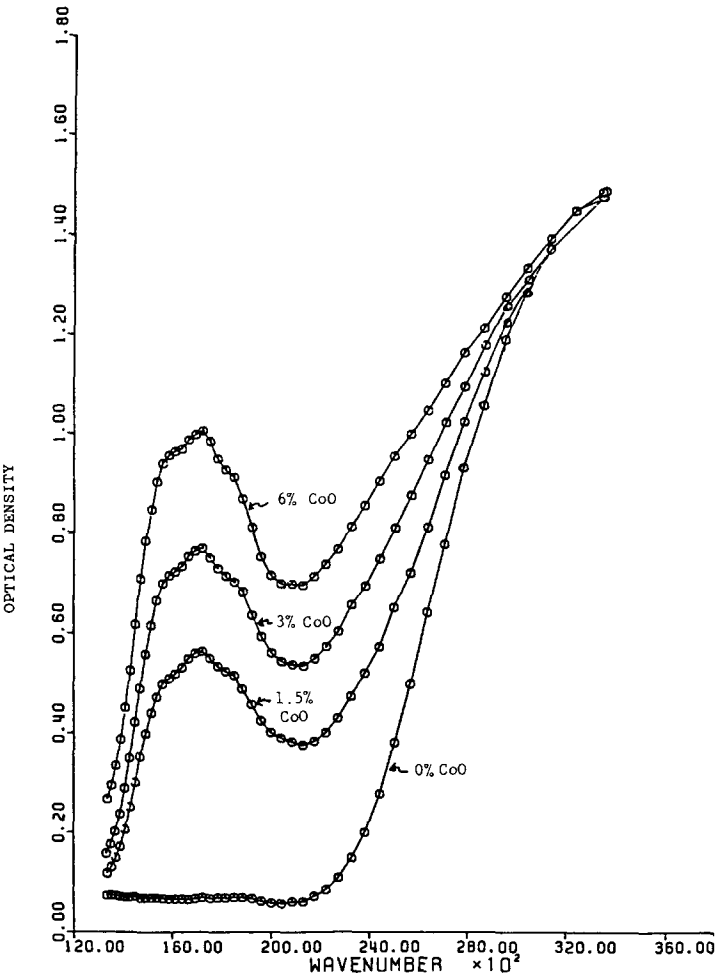

FIG. 4. UV-VIS reflectance spectra of Co/18% MoO_3/alumina.

reasonable. One would therefore expect the deposition of a monolayer of MoO_3 to decrease the pore radius of the Catapal alumina by 51/16 = 3 Å. For the low-area support, having 194 m^2/g area, 24% MoO_3 corresponds to 15 $Å^2$ per MoO_3, close to a monolayer. We find a 4-Å difference between the median pore radius of the low-area alumina and the catalysts containing 18–24% MoO_3 on that alumina. All these results are consistent with a model in which the molybdenums are spread out in a monolayer.

The addition of CoO has the same effect as the addition of MoO_3 in reducing surface area and pore volume. That is to say, a catalyst with a specified percentage alumina retains its pore distribution regardless of the Co/Mo ratio. Thus CoO distributes itself as does MoO_3.

Figure 4 shows typical UV-visible reflectance spectra for a series containing 18% MoO_3, with varying %CoO. The shapes of the spectra around 17.2 kK are the same for all the Co-containing catalysts. The peak represents Co(+2) in tetrahedral coordination. The intense peaks to the right are charge-transfer bands associated with MoO_3. Since the 17.2-kK peak is due to Co, the optical density increases with increasing CoO content, as expected (Fig. 5). However, MoO_3 loading has an effect on

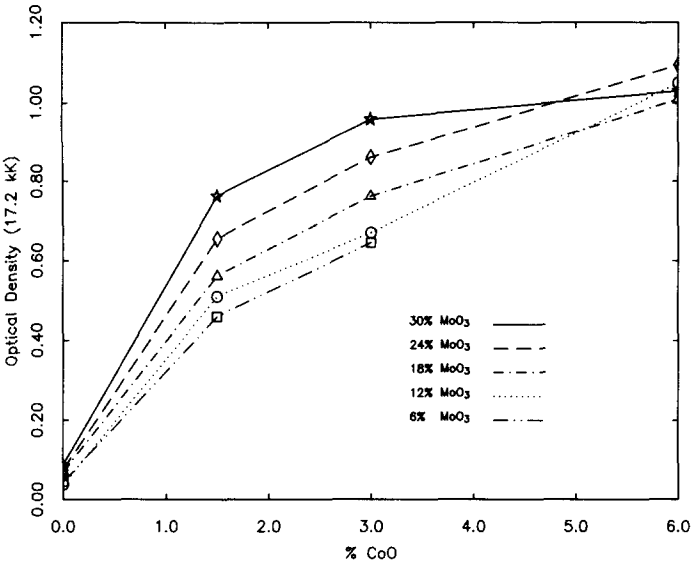

FIG. 5. Reflectance spectra–optical densities for various CoO/MoO_3/Catapal alumina compositions.

this peak intensity, but only in the presence of Co. This is a clear indication that the Co and Mo interact. In the original monolayer model, Schuit and Gates (*4*) proposed that most of the Co resided within the alumina. The present work demonstrates that a significant fraction of the Co does not. In a recent publication Topsøe and Topsøe (*5*) showed, from IR spectra of adsorbed NO, that an interaction between Co and Mo exists in catalysts such as these, and that after sulfiding the Co congregates predominantly at the peripheries of MoS_2 rafts.

The optical density (OD) at 13.5 kK is the lowest in the spectral range available for this series of catalysts. Accordingly, its value is the only measure of the degree to which the backgrounds are raised by the presence of a "black" substance. In many instances, the black substance is carbonaceous material, but in the present series the OD at 13.5 kK (R_c) was taken as a measure of the presence of free cobalt oxide, such as Co_3O_4. In addition, Raman spectroscopy has confirmed the presence of Co_3O_4 in the catalysts which have 12% or more of CoO (*6*). Figure 6 shows that R_c increases logarithmically with increasing CoO content. At the 12% CoO level, the catalysts are visibly darker, with blotches of black.

B. Hydrodesulfurization Activities: Catapal Series

Typical data which show the relationship between WHSV and the degree of desulfurization are presented in Fig. 7. The slopes of these plots are the k values, derived from Eq. (2).

Figure 8 shows how the rate constants at 343°C vary with CoO and MoO_3 content. At a given CoO level, the activity increases with increasing MoO_3. The slopes decrease as MoO_3 increases, so that the activity appears to approach a limiting value at high MoO_3 levels. At a given MoO_3 content, the activity first increases when %CoO was raised from 0 to 1.5% to 3 to 6%, but then markedly decreased at 12% CoO. The observation that the HDS activity passes through a maximum as a function of %CoO has been reported in the literature many times, usually with reference to HDS of a pure compound, such as thiophene; for example, Wivel *et al.* (*7*) and Grange (*8*). Such data have usually been reported in the form of activity vs the ratio Co/Mo, or the

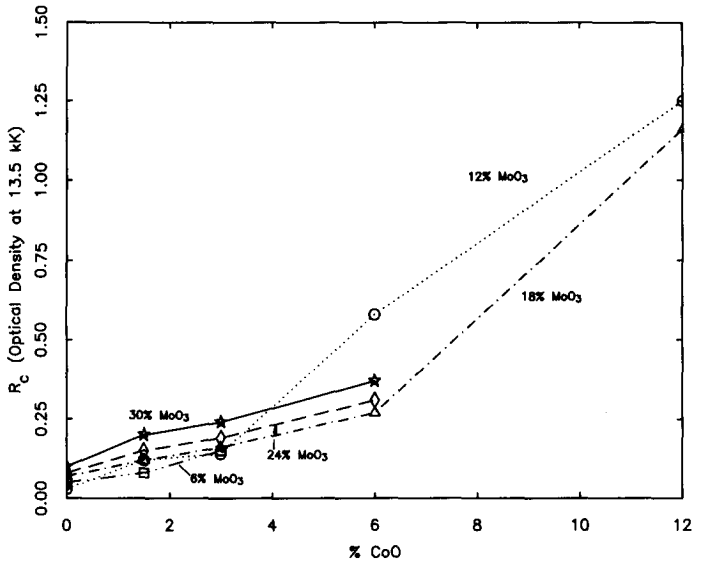

FIG. 6. Optical densities at 13.5 kK for various compositions.

ratio Co/(Co + Mo), even though only a single level of Mo was tested.

The curves drawn in Fig. 8 were derived from an empirical correlation. The (activity/area) was assumed to be the product of three factors:

$$\kappa \equiv k/A = (F_c)(F_i)(F_m), \qquad (3)$$

where $F_c = a + b(\%CoO)$, represents a linear increase in activity with CoO content; $F_m = (\%MoO_3)/[1 + c(\%MoO_3)]$, represents an asymptotic approach to maximum activity at high MoO_3 content; $F_i = 1 - d(\%CoO)$ represents the inhibiting effect of cobalt; A = surface area; a, b, c, and d are constants. The resulting equation is para-

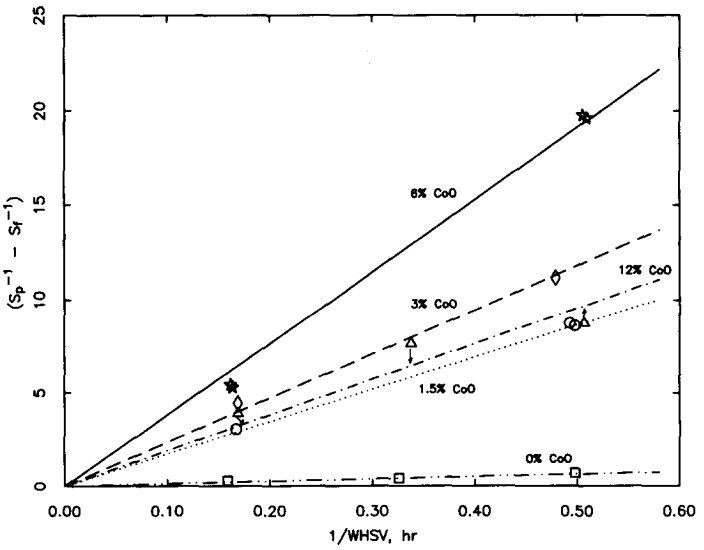

FIG. 7. HDS conversions vs space-time; nominal 18% MoO_3 catalysts. Data taken at 343°C; reaction order: 2.

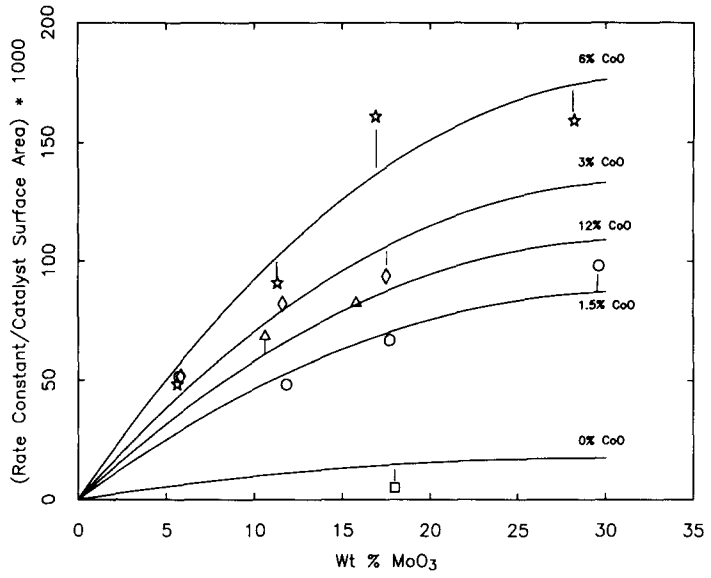

FIG. 8. HDS activity vs molybdenum loading for a range of Co contents. Data taken at 343°C; reaction order: 2.

bolic in %CoO, thus it formally incorporates a maximum. The standard error between the observed k/A values and those predicted by the correlation is 0.016.

At high %CoO levels, the presence of at least some of the Co as the free oxide, in however rudimentary a form, can account for the lack of increased activity, but it cannot account for an inhibiting effect. It is suggested in the accompanying paper (*3*) that excess CoO leads to HDS activity loss by virtue of its effect on the reduction of distortion of the fields around the Mo atoms.

There is a *parallelism* between the EXAFS results for the oxidized catalysts and the HDS activities in the sulfided state. At the nominal 6% MoO_3 level, Table 2 shows no difference in HDS activity on going from 1.5 to 6% CoO. Correspondingly, the differences in apparent first-shell coordination numbers are small in the oxidized state (*1*). At 12 and 18% MoO_3, HDS activity increases and attains a maximum at 6% CoO, and the EXAFS data show a maximum at the same concentration (*1*).

In Table 2, in addition to the catalyst activity data for the Catapal-based series, the results of sulfur analyses of the catalysts after removal from the reactor are also listed. The care taken to protect against air oxidation by storage over argon was buttressed by the protective coating of carbonaceous deposit, and of unpurged oil. The analyses were corrected to the ignited weight basis, as was used for expressing %CoO and %MoO_3. Most of the ignition losses were due to carbon, the analyses for which varied between 4 and 25%. Also shown are values for %S calculated on the assumption of complete conversion to MoS_2 and Co_9S_8. For the most part, the observed analyses are a little below values expected for complete conversion to sulfides, in agreement with the EXAFS results which show that sulfiding is not complete (*3*). The average value of observed-to-predicted ratio is 0.95, with an estimated standard deviation of 0.15. The scatter is probably related to the relatively large corrections to ignited weight basis, and possibly to some sulfur in the carbonaceous deposits.

The catalysts removed from the reactors

TABLE 3

Other HDS Catalysts

History	Catalyst type: Nalcomo 477			Low-area alumina base Virgin
	Virgin	Lab. HDS test + lab. regen.	Commercial use + lab. regen.	
Composition				
%CoO	3.7	3.7	3.3	3.0
%MoO_3	14.9	14.9	14.4	17.5
Surface area (m^2/g)	267	257	191	167
HDS activity				
k (h^{-1})	30.7	30.9	11.9	28.7
$\kappa \equiv k$/Area				
Observed	0.115	0.120	0.062	0.172
Predicted[a]	0.103	0.103	0.103	0.098
% Sulfur[b]				
Observed[c]	N.A.	7.4	6.1	7.8
Predicted[d]	7.5	7.5	7.3	8.7
Ratio	—	0.99	0.8	0.90

[a] Predicted by the correlation derived from the Catapal series.

[b] Analyses of catalysts after HDS testing; expressed on ignited weight basis.

[c] By LECO method.

[d] Assuming conversion to Co_9S_8 + MoS_2.

after the activity tests were examined by EXAFS, as described in (*3*), where they have been designated as Group IV samples.

C. Hydrodesulfurization Activities: Other Catalysts

HDS activities and compositions of several catalysts not part of the series based on Catapal alumina are listed in Table 3. The activities predicted by the above correlation for the Catapal series were also included. The HDS activity of the virgin Nalcomo 477 catalyst is very close to that predicted for a member of the Catapal series with the same CoO/MoO_3 content. Its activity did not change when the catalyst was regenerated after a 2-week activity run, and then retested. The apparent first-shell coordination number for Mo is also the same as for the Catapal series in the oxidized state (*1*), which indicates that the state of Mo for the Nalcomo and the Catapal series are the same in the oxidized state.

The sample of Nalcomo 477 taken after extended use in a commercial unit and subjected to laboratory regeneration has an HDS activity only 39% of that observed for the virgin catalyst. This is typical of commercially used and regenerated HDS catalysts. On a unit area basis, the activity is 54% of the activity observed for the virgin catalyst, and 60% of the predicted value. The corresponding EXAFS data showed that the coordination of oxygen atoms about the Mo's in the regenerated catalyst (before sulfiding) was not the same as in the virgin catalyst (*1*). Also, the relative area of the resolved A_3 peak (assigned to the $1s \rightarrow 5p$ transition) is lower than that of the virgin catalyst, which in turn is the same as that for a Catapal-based catalyst of the same composition. Again, there is a parallelism between EXAFS results in the oxidized state and the HDS activity in the sulfided state. On the other hand, the differences are small between the apparent first-shell

coordination numbers (Mo–O) of virgin or regenerated Nalcomo 477 and a Catapal-based catalyst of the same composition.

On a weight basis, the low-area alumina catalyst has an activity (Table 3) which is 22% higher than that of a Catapal-based catalyst of the same composition (Table 2). On an area basis, it is 82% higher. On the other hand, the activity per unit area of XCAT is 35% lower than that of a Catapal-based catalyst of the same composition. The EXAFS results in the oxidized state show little difference in the Mo–O coordination between the catalysts based on Catapal and that based on the low-area alumina, when the promoter contents are expressed on an area basis (*1*). Those data provide no explanation of HDS activity differences.

FURTHER COMMENTS ON ACTIVITY

It is well established that catalytic activity is closely related to the concentration of the metals in the catalysts (*8*). Increasing the promoter content initially raises the activity; then after attaining a maximum the activity decreases upon further addition of the promoter. Others (*7, 9*) suggested that the catalytic activity is proportional to the amount of Co present as Co–Mo–S. When the amount of Co exceeds a specified limit, a new phase appears (Co_9S_8), and it is presumed that this covers some of the active sites.

It has been proposed the HDS activity is associated with anion vacancies (*10*). In the simplest model such vacancies are located predominantly at the edges of platelets where the Mo atoms are incompletely coordinated to sulfur or oxygen atoms. Also it has been proposed that the Co atoms congregate at these perimeters. Hence the larger the totality of perimeters, i.e., the smaller the platelets, the greater the activity. To relate the measured activities to the structural data, introduced the assumption that the measured rate constant per unit area of catalysts is proportional to the number of Mo–S pairs (or Mo–Mo pairs) located at the *rims* of the platelets. In the accompanying paper that number was estimated from the measured RD peak areas derived from EXAF spectra (Eq. (7) in Ref. (*3*)):

$$\#(\text{Mo–S})_{\text{rim}} = \alpha\left\{\tfrac{2}{3}N_t \frac{c_2^2}{c_1}\frac{D}{W^2}\right\}^{1/2}\left\{SA * \rho * [\text{Mo}]\frac{A(\text{Mo–S})}{2648}\right\}^{1/2}. \quad (4)$$

The first brace incorporates terms which are controlled by the time–temperature history of the catalyst, as well as by its Co loading; it corresponds to the product $(F_c)(F_i)$ of Eq. (3) which empirically accounts for the dependence of activity on Co content. At this time we have no structural data pertaining to these factors. The second brace includes the surface area (SA), the density, the number of Mo's per unit volume, and the conversion ratio. Hence the predicted dependence on Mo content (but modulated by Co) is

$$\kappa * SA * \rho \Leftrightarrow \left\{SA * \rho * [\text{Mo}]\frac{A(\text{Mo–S})}{2648}\right\}^{1/2}. \quad (5)$$

[The product $(SA * \rho)$ must be inserted in the left member for dimensional consistency.] This correlation for 12 HDS laboratory tested samples is plotted in Fig. 9a; κ vs $G * Y_S$, where G is a convenient scale factor and $Y_S \equiv \left\{[\text{Mo}]\frac{A(\text{Mo–S})}{2648}\right\}^{1/2}$; here [Mo] is moles of Mo/100 g of catalyst/unit area. The standard error is 0.0162. If one assumes that pairs of adjacent (Mo–Mo)'s at the rim of platelets are required for catalysis, then the corresponding parameter is $Y_M \equiv \left\{[\text{Mo}]\frac{A(\text{Mo–Mo})}{6337}\right\}^{1/2}$, and the standard error is slightly lower [0.0155], but this improvement is not sufficient for demonstrating that Mo–Mo pairs, rather than Mo–S, comprise the crucial structural feature. When the four commercial preparations and the low-A sample were included, the standard error (vs Y_M) rose to 0.0237 (0.0239 vs Y_S) (Fig. 9b). Clearly, the presence of the promoter and the preparative

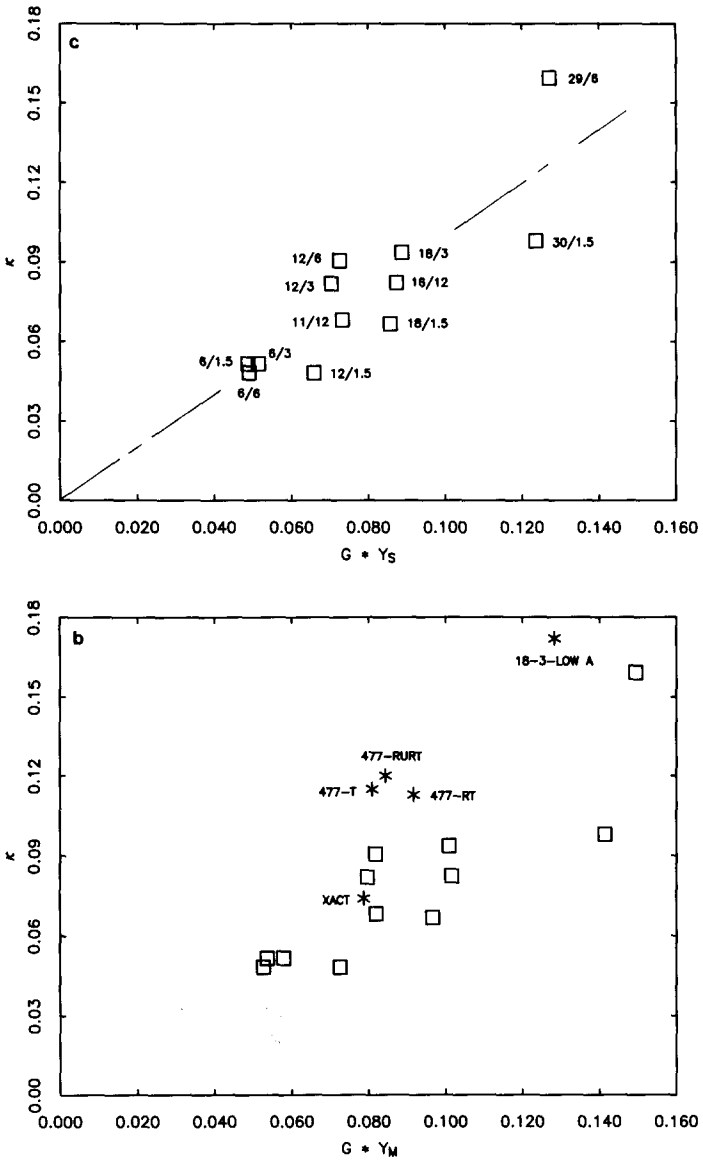

FIG. 9. HDS rate constant/unit area of catalyst vs Y_S: (a) for 12 samples; and Y_M (b) for 17 samples (*3*).

history of the sample moderate the direct dependence of activity on structure. Our concurrent exploration of the structure of the Co species via their K-edge spectra may lead to more specific models. To our knowledge this is the first *direct* demonstration that a structural feature, the presence of Mo–Mo or Mo–S rim-pairs, is the effective unit for catalysis (*11*).

ACKNOWLEDGMENTS

This work was supported by a grant from the ARCO Petroleum Products Company, a division of Atlantic Richfield Company. The catalysts were prepared by Mr. R. W. Tumbula, and the HDS activity data were obtained by Mr. C. K. Kim, both of ARCO.

REFERENCES

1. Chiu, N-S., Bauer, S. H., and Johnson, M. F. L., *J. Catal.* **89**, 226 (1984).

2. Chiu, N-S., Bauer, S. H., and Johnson M. F. L., *J. Mol. Struct.* **125,** 33 (1984).
3. Chiu, N-S., Bauer, S. H., and Johnson, M. F. L., *J. Catal.* **98,** 32 (1986).
4. Schuit, G. C. A., and Gates, B. C., *AIChe J.* **19,** 417 (1973).
5. Topsøe, N-Y., and Topsøe, H. *J. Catal.* **75,** 354 (1982).
6. Baney, H. F., private communication.
7. Wivel, C., Candia, R., Clausen, B. S., Mørup, S., and Topsøe, O. H., *J. Catal.* **68,** 453 (1981).
8. Grange, P., *Catal. Rev.-Sci. Eng.* **21,** 135 (1981).
9. (a) Topsøe, H., Clausen, B. S., Candia, R., Wivel, C., and Mørup, S., *J. Catal.* **68,** 433 (1981); (b) Alstrup, I., Chorkendorff, I., Candia, R., Clausen, B. S., and Topsøe, H., *J. Catal.* **77,** 397 (1982).
10. (a) Lipsch, J. M. J., and Schuit, G. C. A., *J. Catal.* **15,** 163, 174, 179 (1969); (b) Taustu, S. G., Pecoraro, T. A., and Chianelli, R. R., *J. Catal.* **63,** 515 (1980); (c) Desikan, P., and Amberg, C. H., *J. Canad. Chem.* **42,** 397 (1982).
11. Kasztelan, S., Toulhoot, H., Grimblot, J., and Bonnelle, J. H., *Bull. Soc. Chim. Belg. 91/n,* 807 (1984).